JOURNAL OF MATERIALS SCIENCE **38** (2003) 1849–1852

Viscoelasticity and relaxation characteristics of polystyrene/clay nanocomposite

J.-I. SOHN
Department of Chemistry, Hallym University, Chunchon 200-702, Korea
E-mail: jisohn@hallym.ac.kr

C. H. LEE, S. T. LIM, T. H. KIM, H. J. CHOI
Department of Polymer Science and Engineering, Inha University, Incheon 402-751, Korea
E-mail: hjchoi@inha.ac.kr

M. S. JHON
Department of Chemical Engineering, Carnegie Mellon University, Pittsburgh, PA 15213-3890, USA

Polymer nanocomposites based on an organophilically modified montmorillonite (OMMT) and polystyrene (PS) are prepared via a solvent casting method using chloroform as a cosolvent to examine their dynamic viscoelastic and relaxation properties, in which the increased basal spacings of the OMMT determined by X-ray diffraction indicated the intercalation of PS chains into OMMT interlayer. From the measured viscoelastic properties originated from the nanocomposite interaction between polymer and OMMT, we were able to determine the characteristic behavior of PS/OMMT nanocomposites. Storage and loss moduli are found to give the transition from liquid-like to solid-like behavior as the clay content increases, especially in the low frequency region. Stress relaxation behavior was also enhanced by showing more solid-like characteristics with increasing OMMT.

1. Introduction

Polymer/clay nanocomposites have recently attracted considerable attention, primarily due to enhanced material properties via nanoscale reinforcement in contrast to the conventional particulate filled, microcomposites [1, 2]. These nanocomposites exhibit an increased modulus [3–5], reduced gas permeability [6], enhanced thermal stability, and self-extinguishing fire-retardant characteristics [7, 8]. For example, the doubling of the tensile modulus and increase in the heat distortion temperature up to 100°C for nylon/clay nanocomposites with as little as 2 vol% of inorganic content [9] are achieved. Biodegradable polymer based nanocomposites have been also recently developed [10–12].

Investigations for polymer/clay nanocomposites are extended even further to various applications, such as electrorheological (ER) fluid consisting of a suspension of micron-sized particles and electrically conducting materials [13, 14]. This kind of application exhibits drastic and reversible changes in the rheological properties in the presence of an external electric field [15–18]. As another investigations, VanderHart *et al*. [19] examined the characteristic formation of α-phase crystallites in polymer/clay nanocomposite, which preferentially exist near the nylon/clay interfaces. Kim *et al*. [20] also showed that organic/inorganic hybrid core-shell nanoparticles can be used as a promising nanostructural building block, leading to ordered ultra thin nanocomposites films having good mechanical strength, chemical resistance, thermal stability, and a barrier property through layered architecture and the ionic interaction with the cationic polyelectrolytes.

The rheological properties of polymer/clay nanocomposites are determined by a combination of the mesoscopic structure and the strength of the interaction between the polymer and clay. The mesoscopic structure depends not only on the strength of polymer/clay interaction but also on the inherent viscoelastic properties of the matrix in which the clay layers are dispersed. Due to this kind of internal structure, polymer/clay nanocomposites have provided important characteristics of the static and dynamic properties of confined polymer including viscoelastic properties [1, 5, 21, 22].

As one of the most widely used commodity plastic materials, polystyrene (PS) has been modified to enhance mechanical and thermal properties in many different ways. Since Friedlander and Grink [23] observed a slight expansion of the d_{001}-spacing of clay galleries upon PS intercalation, PS/clay nanocomposites have been widely investigated. Zhu *et al.* [8] prepared intercalated and exfoliated PS/clay nanocomposites using a bulk polymerization technique. In their study, they showed by using thermo-gravimetric analysis that the onset of thermal degradation occurs at a higher temperature for the nanocomposites than for the virgin

polymer [8]. Hoffman *et al*. [24] prepared fully exfoliated PS nanocomposites containing silicate nanoparticles. Both the PS continuous matrix and the ammonium-terminated PS attached to the silicate nanoparticle surface exhibited very narrow molecular weight distributions, therefore, it became possible to correlate superstructure formation with rheological properties. Recently we also synthesized PS/clay nanocomposites by the emulsion polymerization of styrene in the presence of sodium ion-exchanged montmorillonite (Na^+-MMT) and found more pronounced shear thinning behavior with increasing clay content [25].

In this work, we investigated the viscoelastic properties and stress relaxation of PS/OMMT nanocomposites. The internal structure of PS/OMMT nanocomposites was elucidated using the XRD. The viscoelastic properties, which are obtained via oscillatory shear using a parallel plate geometry rheometer, gave much information to explain the flow behavior and suspension microstructures.

2. Experimental

2.1. Materials and PS/clay nanocomposites preparation

The PS (M_w = 230,000 g/mol) was purchased from Aldrich Chemical Co (USA). The OMMT (Cloisite 25A) obtained from Southern Clay Product (Gonzales, Texas, USA) was used without any treatment. The pristine Na^+-MMT has been treated organophilically by cation exchange reaction with a dimethyl, hydrogenated tallow (composed of about 65% octadecyl chains, about hexadecyl chains and about 5% C_{14} alkyl chains), and 2-ethylhexyl, quaternary ammonium methylsulfate. The cationic exchange capacity of OMMT (oganophilic-MMT) is 95 meq/100 g clay, and the interlayer spacing is 1.942 nm, which is measured by XRD.

The nanocomposites were prepared via solvent casting. Both the PS and OMMT were dried in a vacuum oven to remove moisture. PS (29.4 & 27 g) and OMMT (0.6 & 3 g) were dissolved/dispersed in chloroform (400×10^{-6} m^3) at 25°C using a magnetic stirrer, for 1 day. After mixing the PS solution and OMMT dispersion together, the mixture was stirred for 2 additional days. The chloroform was then evaporated in a hood, and all of the samples were subsequently dried to constant weight in a vacuum oven for 1 day. The sample code was designated as PS, PSM2, PSM10 according to the ratio of PS/OMMT; 100/0, 98/2, 90/10. The disk type samples of these nanocomposites having 2.18 mm thickness and 18 mm diameter were prepared using a hot press (Caver, Model 3852, Wabash, USA) at 140°C for rheometer test.

2.2. Characterization

The increase of interlayer distance of OMMT in the nanocomposites was studied via XRD, whose patterns were monitored with a Guinier focusing camera using a Philips X-ray crystallographic unit (PW-1847), running at 40 kV and 50 mA. Scanning angle (2θ) ranged from 1.5° to 10° at the rate of 3°/min. To measure rheological properties, a rotational rheometer (Physica, MCR 300, Germany) with a parallel plate geometry was used. The plates (25 mm diameter) were separated in 1.0 mm gap distance at a fixed temperature of 200°C. Storage and loss moduli were obtained in a melt state as a function of frequency. We fixed the amplitude at 0.3% by strain sweep. To obtain these dynamic properties, a time dependent oscillatory stain of the form, $\gamma(t) = \gamma_0 \sin(\omega t)$, was applied, in which γ_0 is the strain amplitude, ω is the frequency (varied from 0.001 to 100 rad/s) and t is time. The resulting time-dependent shear stress ($\tau(t)$) is of the following form

$$\tau(t) = \gamma_0[G' \sin(\omega t) + G'' \cos(\omega t)] \qquad (1)$$

Here, G' is the storage or elastic modulus and G'' is the loss or viscous modulus. The linearity of measurements is typically confirmed by repeating the measurement at higher and lower strain amplitudes and observing the independence of the measured G' and G'' moduli. The slopes of the G' and the G'' versus the ω in the terminal region were smaller than 2 and 1, respectively [5].

3. Results and discussion

Fig. 1 shows the XRD patterns of PS/OMMT nanocomposites. We estimated the variation of the d_{001} spacing, which is obtained from the observed peaks of the angular position (2θ) according to the Bragg formula ($n\lambda = 2d \sin\theta$). The d-spacing of OMMT increased from 1.94 nm to 3.27 nm. The change in d-spacing indicates that PS was intercalated into the OMMT interlayers [5, 26]. Meanwhile, the maximum peak intensities of PSM2 and PSM10 locate at the same angular positions, suggesting that d-spacing for the PS/OMMT nanocomposites is independent of the OMMT loading. Similar behaviors have been already examined by other researchers [5, 21, 26, 28], only giving rise to the variation of relative peak intensities.

Linear viscoelastic responses, such as storage modulus (G') and loss modulus (G''), are shown in Fig. 2a and b, respectively. These data sets were acquired at the

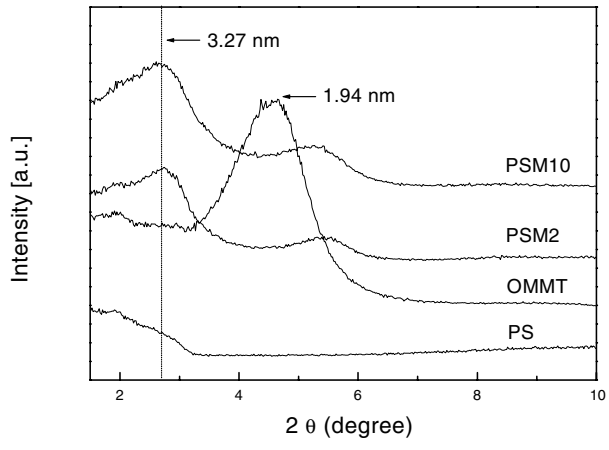

Figure 1 The XRD spectra of the PS, OMMT, and PS/OMMT nanocomposites.

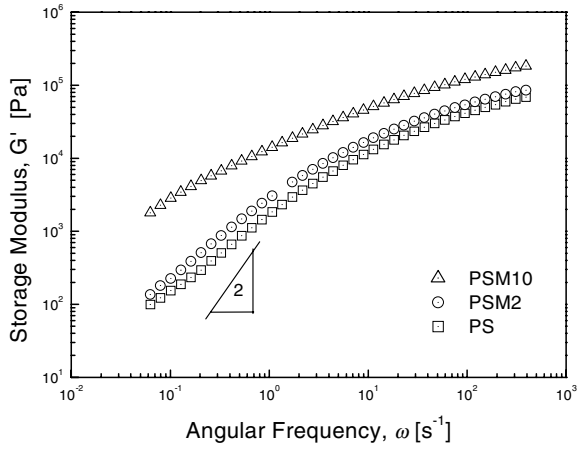

(a)

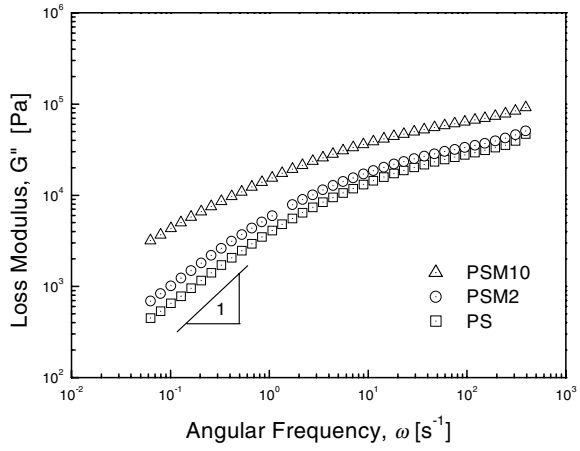

(b)

Figure 2 Storage (a) and loss (b) moduli of PS and PS/OMMT nanocomposites at 200°C.

strain of 0.3% in 0.01–100 Hz frequency range. Both G' and G'' show monotonic increase in the entire frequency range with the increase in silicate loading. Especially, the slope in the low frequency region decreases with the clay content. Implying that the flow properties in this region change to more solid-like type due to the addition of OMMT, which promotes OMMT/polymer interaction. This result agrees well with our previous results on the PEO/clay nanocomposite system [5].

The G' has slopes of 0.94, 0.94, and 0.62 (for PS, PSM2, PSM10) while G'' has slopes of 0.62, 0.62, and 0.46 (for PS, PSM2, PSM10) in log plots, indicating that at the lowest frequencies, the response of the system exhibits liquid-like behavior ($G'' > G'$). However, the two moduli soon become equal and display nearly a plateau region, having higher G' than G''. In this region, PS/OMMT nanocomposites show glassy solid-like behavior [29]. This characteristic transition (from liquid-like to solid-like behavior) shifts to the low frequency region as the OMMT loading increases. The crossover points occur at 14.8, 11.0 and 2.22 rad/s for PS, PSM2 and PSM10, respectively. Therefore, with increasing OMMT loading, nanocomposite systems exhibit more rapid solid-like behavior in the entire frequency range [30]. This solid-like behavior can be explained with the decrease of slope in G' [21, 30]. The slopes and the absolute values of the dynamic moduli indicate a supermolecular structure formation in the nanocomposites. It means that the higher the G' and the smaller the slope implies more pronounced intercalation between the silicate platelets and their tendency to form a three-dimensional superstructure. The end-tethered polymer chains on the silicate layers stabilize this superstructure [30].

Fig. 3 shows G' vs. G'' plots in log scale for PS and PS/OMMT nanocomposites with different OMMT contents. This plot is refered to as modified Cole-Cole plot [31, 32]. This plot suggests that the homogeneous polymer blends exhibit temperature independent behavior in modified Cole-Cole plot [33]. In Fig. 3 both PS and PS/OMMT nanocomposites show similar behavior, having the slope of 2. Therefore, it can be said that PS and PS/OMMT nanocomposite systems maintain the homogeneities for different OMMT loadings. In other words, OMMT loadings do not affect the morphological state of PS/OMMT nanocomposites.

Fig. 4 shows stress relaxation of PS and PS/OMMT nanocomposites. Stress relaxation modulus $G(t)$ describes a time dependent response after a shear step.

$$G(t) = \tau(t)/\gamma_0 \tag{2}$$

To obtain the $G(t)$, viscoelastic material is instantly deformed to a shear strain γ_0. While this deformation

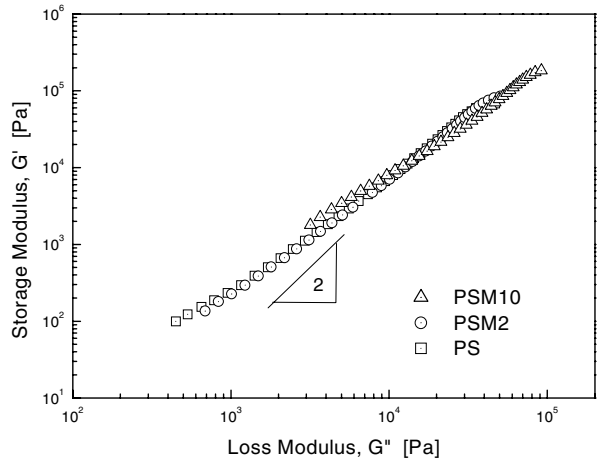

Figure 3 Modified Cole-Cole plot (G' vs. G'') of the PS and PS/OMMT nanocomposites.

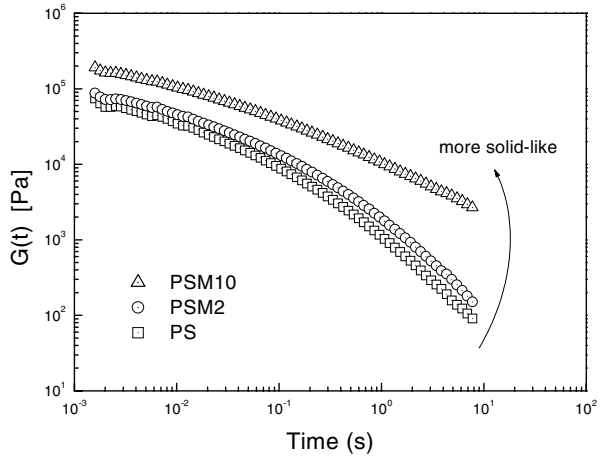

Figure 4 Shear stress relaxation curve obtained using Schwarzl method [30, 31] for PS and PS/OMMT nanocomposites.

is maintained, the stress is measured as a function of time. $G(t)$ can also be measured by oscillatory experiment, and the result compared with that obtained from the previously mentioned method. In most cases, the larger molecules have longer relaxation times and smaller ones have shorter relaxation times.

In this study, the $G(t)$ was calculated via the Schwarzl methods [34, 35] from the G' and G'' data obtained from the dynamic oscillatory shear test.

$$G(t) = [G'(\omega) - 0.560G''(\omega/2) + 0.200G''(\omega)]_{\omega=1/t} \quad (3)$$

From the measurements in a variety of homopolymer melt systems, one found that the nonlinear shear relaxation modulus $G(t, \gamma)$ can be factorized into a linear relaxation modulus $G(t)$ and a damping function $h(\gamma)$:

$$G(t, \gamma) = G^0(t)h(\gamma) \quad (4)$$

The time range of $G(t)$ limits the time range of the G' and G''. Low frequencies correspond to very large relaxation times, and vice versa. This means that the best result will be obtained from a long time of the input data and a limited frequency range of the output data. Note that Ren *et al.* [36] studied the linear stress relaxation of PS-polyisoprene (PI) block copolymer/clay nanocomposites by using a two-point collocation method. In Fig. 4, the liquid-like stress relaxation modulus, observed for the unfilled polymer, gradually changes to solid-like behavior as OMMT content increase [21].

4. Conclusions

Viscoelastic and relaxation properties of intercalated PS/OMMT nanocomposites prepared via solvent casting are examined. The chain insertion into OMMT is verified from XRD patterns, which show the increase of interlayer spacing. Both storage modulus and loss modulus of PS/OMMT nanocomposites increase and exhibit non-terminal behavior, as the OMMT contents increase. From the viscoelastic measurement, we show that PS/OMMT system is more solid-like than PS. In addition, OMMT loadings do not affect the homogeneities of the PS/OMMT nanocomposites systems.

Acknowledgments

This study was supported by Hallym Academy of Sciences, Hallym Univeristy, Korea (2003-18-1).

References

1. E. P. GIANNELIS, R. KRISHNAMOORTI and E. MANIAS, *Adv. Polym. Sci.* **138** (1999) 107.
2. M. ALEXANDRE and P. DUBOIS, *Mater. Sci. Eng.* R **28** (2000) 1.
3. S. K. LIM, J. W. KIM, I. CHIN, Y. K. KWON and H. J. CHOI, *Chem. Mater.* **14** (2002) 1989.
4. Z. WANG and T. J. PINNAVAIA, *ibid.* **10** (1998) 1820.
5. Y. H. HYUN, S. T. LIM, H. J. CHOI and M. S. JHON, *Macromolecules* **34** (2001) 8084.
6. P. B. MESSERSMITH and E. P. GIANNELIS, *J. Polym. Sci. Part A: Polym. Chem.* **33** (1995) 1047.
7. F. DIETSCHE and R. MÜLHAUPT, *Polym. Bulletin* **43** (1999) 395.
8. J. ZHU, A. B. MORGAN, F. J. LAMELAS and C. A. WILKIE, *Chem. Mater.* **13** (2001) 3774.
9. A. USUKI, M. KAWASUMI, Y. KOJIMA, A. OKADA, T. KURAUCHI and O. KAMIGAITO, *J. Mater. Res.* **8** (1993) 1174.
10. S. T. LIM, Y. H. HYUN, H. J. CHOI and M. S. JHON, *Chem. Mater.* **14** (2002) 1839.
11. M. A. PAUL, M. ALEXANDRE, P. GEGÉE, C. HENRIST, A. RULMONT and P. DUBOIS, *Polymer* **44** (2003) 443.
12. G. X. CHEN, G. J. HAO, T. Y. GUO, M. D. SONG and B. H. JHANG, *J. Mater. Sci. Lett.* **21** (2002) 1587.
13. B. H. KIM, J. H. JUNG, J. W. KIM, H. J. CHOI and J. JOO, *Synth. Met.* **117** (2001) 115.
14. B. H. KIM, J. H. JUNG, J. JOO, A. J. EPSTEIN, K. MIZOGUCHI, J. W. KIM and H. J. CHOI, *Macromolecules* **35** (2002) 1419.
15. J. W. KIM, S. G. KIM, H. J. CHOI and M. S. JHON, *Macromol. Rapid. Commun.* **20** (1999) 450.
16. J. W. KIM, M. H. NOH, H. J. CHOI, D. C. LEE and M. S. JHON, *Polymer* **41** (2000) 1229.
17. H. J. CHOI, J. W. KIM, J. JOO and B. H. KIM, *Synth. Met.* **121** (2001) 1325.
18. J. W. KIM, F. LIU and H. J. CHOI, *J. Ind. Eng. Chem.* **8** (2002) 399.
19. D. L. VANDER HART, A. ASANO and J. W. GILMAN, *Chem. Mater.* **13** (2001) 3796.
20. D. W. KIM, A. BLUMSTEIN and S. K. TRIPATHY, *ibid.* **13** (2001) 1916.
21. H. SHI, T. LAN and T. J PINNAVAIA, *ibid.* **8** (1996) 1584.
22. H. J. CHOI, S. G. KIM, Y. H. HYUN and M. S. JHON, *Macromol. Rapid. Commun.* **22** (2001) 320.
23. H. Z. FRIEDLANDER and C. R. GRINK, *J. Polym. Sci., Polym. Lett.* **2** (1964) 475.
24. B. HOFFMANN, C. DIETRICH, R. T. THOMANN, C. FRIEDRICH and R. MÜLHAUPT, *Macromol. Rapid Commun.* **21** (2001) 57.
25. T. H. KIM, L. W. JANG, D. C. LEE, H. J. CHOI and M. S. JHON, *ibid.* **23** (2002) 191.
26. J. ZHU and C. A. WILKIE, *Polym. Int.* **49** (2000) 1158.
27. R. A. VAIA and E. P. GIANNELIS, *Macromolecules* **30** (1997) 7990.
28. R. A. VAIA, K. D. JANDT, E. J. KRAMER and E. P. GIANNELIS, *ibid.* **28** (1995) 8080.
29. R. K. GUPTA, "Polymer and Composite Rheology" (Marcel Dekker, New York, 2000).
30. B. HOFFMANN, J. KRESSLER, G. STÖPPELMANN, C. FRIEDRICH and G. M. KIM, *Colloid. Polym. Sci.* **278** (2000) 629.
31. E. R. HARELL and N. NAKAJIMA, *J. Appl. Polym. Sci.* **29** (1984) 995.
32. P. J. YOON and C. D. HAN, *Macromolecules* **33** (2000) 2171.
33. C. D. HAN and M. S. JHON, *J. Appl. Polym. Sci.* **32** (1986) 3809.
34. F. R. SCHWARZL, *Rheol. Acta* **10** (1971) 166.
35. *Idem.*, *ibid.* **14** (1975) 581.
36. J. REN, A. S. SILVA and R. KRISHNAMOORTI, *Macromolecules* **33** (2000) 3739.

Received 26 December 2002
and accepted 19 February 2003